World Conference on Timber Engineering Oslo 2023

PERFORMANCE OF GLUED-IN RODS IN GLULAM AND MPP IN TENSION AND COMPRESSION

Alexander Salenikovich[1], Étienne Lapointe[2], Bruno Zumbrunn-Maurer[3], Thomas Brotschi[4], Anthonie Kramer[5]

ABSTRACT: This paper is focused on evaluation of the performance of glued-in rods (GIR) in Douglas-fir glulam timber and Mass Ply Panels (MPP) produced in the USA for structural applications. One of the objectives of the study was to compare the performance of GIR joints with and without recess of the bond length in tension and compression. High-strength steel threaded rods of 15.9 mm in diameter were bonded into wood members of 70 mm × 70 mm in cross-section in three configurations. In one configuration, the bond length was 20 times the stress diameter (d_s) of the rod. In another configuration, the embedded length of the rod included a machined portion (constriction zone) near the end of the wood member, which created a recess (not bonded length) of 4d, while the bond length remained the same (20d_s). In the third configuration, the bond length was 24d_s without a recess. Test results clearly demonstrated the benefits of a recess in GIR joints to increase the structural efficiency of timber connections. No GIR buckling was observed in compression tests.

KEYWORDS: Bonded-in threaded rods, GSA Technology, Mass Ply Panel (MPP), splitting, stiffness of GIR joints

1 INTRODUCTION

With growing demand in multistorey mass timber construction, there is a critical need in efficient, reliable, fire-resistant, and aesthetically pleasing connections. Joints with glued-in rods (GIR), if properly designed and executed, meet these requirements. Glued connections are strong and rigid, but due to inherent weaknesses of wood in shear and low splitting resistance, they may provoke undesirable premature brittle wood failures leading to a catastrophic collapse if not taken into account in design. It is desirable to optimize the joints to achieve an equivalent strength and stiffness with the wood structural elements while minimizing the risk of brittle wood failures [1].

Connections with GIR connections have been successfully applied in large-span timber structures in Russia since the 1980s [2], which resulted in the design provisions for GIR [3]. During the last decade, several adhesives for use with GIR systems in timber structures have been developed and approved in Europe [4],[5],[6],[7],[8],[9],[10]. Common rules for the assessment of GIR have been adopted in EU in 2019 [11]. Testing requirements for GIR in glued structural timber products have been adopted in 2021 [12]. Basic provisions for design of GIR for timber connections are now given in EOTA TR 070 [13], and considered in the Eurocode 5 draft [14]. Nowadays, developers seek approval of GIR technologies in North America.

One of the main objectives of this project was to facilitate the development of acceptance criteria for factory installed glued-in rods in wood structural elements to be evaluated for the use in mass timber construction in North America [15]. In addition, the test program was undertaken to compare the performance of GIR in static tension and compression and to demonstrate the advantages of the special rod design used in the GSA Technology.

2 METHODOLOGY

The experimental study was conducted on high-strength steel threaded rods of the class B7 [16] of 15.9 mm (d = 5/8 in.) in diameter bonded at the ends of wood members using the GSA adhesive, a two-component epoxy resin. The high-strength steel was used to minimize the chance of the rod yielding and to force the failure of the bond line or of the wood. The wood members were Douglas-fir glulam timber (GLM) and Mass Ply Panel (MPP) [17] of 70 mm × 70 mm in cross-section. In the first configuration (Series "20d"), the bond length was 267 mm, approximately 20 times the stress diameter (d_s) of the rod. In the second configuration (Series "20d-c"), the embedded length of the rod included a machined portion (constriction zone) near the end of the wood member, which created an additional recess (not bonded length) of 51 mm (14+51 ≈ 4d), while the bond length remained the same (≈ 20d_s). This configuration was representative of the GSA Technology [4]. In the third

[1] Université Laval, Canada, alsal10@ulaval.ca
[2] Université Laval, Canada, etlap6@ulaval.ca
[3] GSA Technology AG, Switzerland, brm@gsa-technology.ch
[4] ASPECT Structural Engineers, thomas@aspectengineers.com
[5] anthoniekramer@gmail.com

https://doi.org/10.52202/069179-0173

configuration (Series "24d"), the bond length was 317 mm (≈ $24d_s$) without a recess. Five specimens were fabricated and tested for each configuration and wood material. The dimensions of steel rods are illustrated in Figure 1. The definitions of the variables are depicted in Figure 3. The values of the variables in each test series are summarized in Table 1.

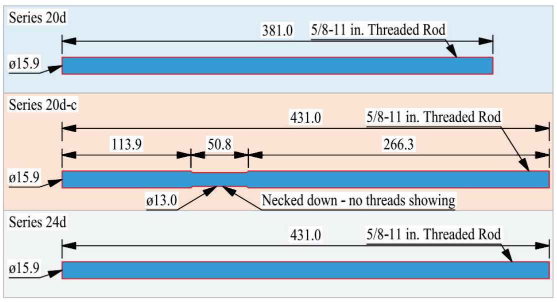

Figure 1: *Dimensions of steel rods*

At first, the specimens were tested in tension by static loading using self-centering pinned fixtures in accordance with ISO 6891 [18] loading procedure until failure at one end. The speed of testing was chosen so to achieve failure within (5 ± 2) minutes. The slip of the joints was measured using three laser-displacement sensors at each end (see Figure 2). The reference plates were glued at the ends of the wood member and the mounting platform for the laser sensors was attached to the ends of the rods with nuts and Belleville washers. The distance between the member end and the mounting platform of the laser sensors was 46 mm in the tension and 26 mm in the compression setup. After the tensile test, the wood member was cut in half, and the surviving joint was tested in compression with a ramp load at the same speed. The load was applied until failure or until the load head reached 15 mm displacement. The maximum load, the slip, the elastic stiffness (slip modulus), and the failure mode were determined for each test. The specific gravity and moisture content of wood members were measured in accordance with ASTM D2395 [19] using full cross-section samples cut near mid-length of each specimen.

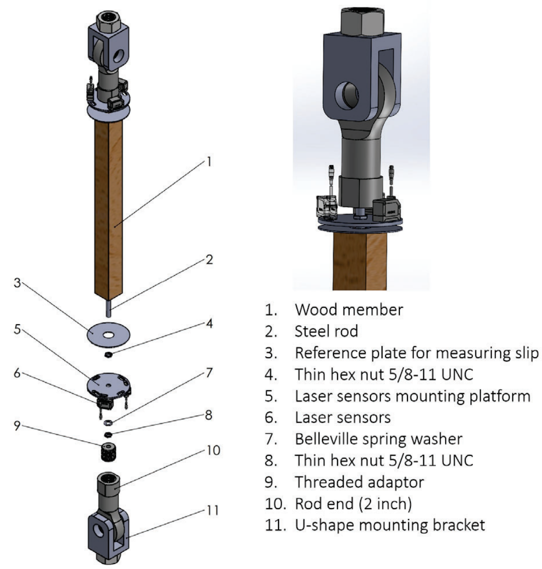

Figure 2: *Tensile load test setup*

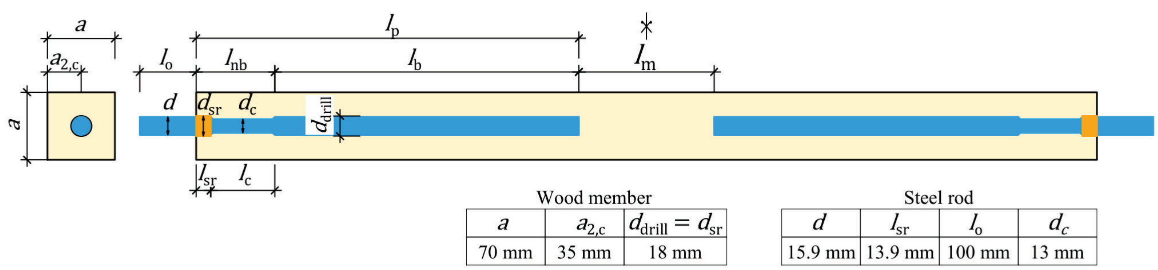

Figure 3: *Definition of GIR parameters*

Table 1: *Variable parameters of GIR joints*

Series[1)]	Load	d_s	Bond length (ℓ_b)		ℓ_c	ℓ_p	ℓ_m
		[mm]	[$\times d_s$]*	[mm]	[mm]	[mm]	[mm]
T-20d	Tension	13.6	20	267	0	281	238
T-20d-c	Tension	13.0	20	266	51	331	138
T-24d	Tension	13.6	24	317	0	331	138
C-20d	Compression	13.6	20	267	0	281	119
C-20d-c	Compression	13.0	20	266	51	331	69
C-24d	Compression	13.6	24	317	0	331	69

* Approximately

[1)] Each configuration was produced with Douglas-fir glulam (GLM) and with Mass Ply Panel (MPP).

https://doi.org/10.52202/069179-0173

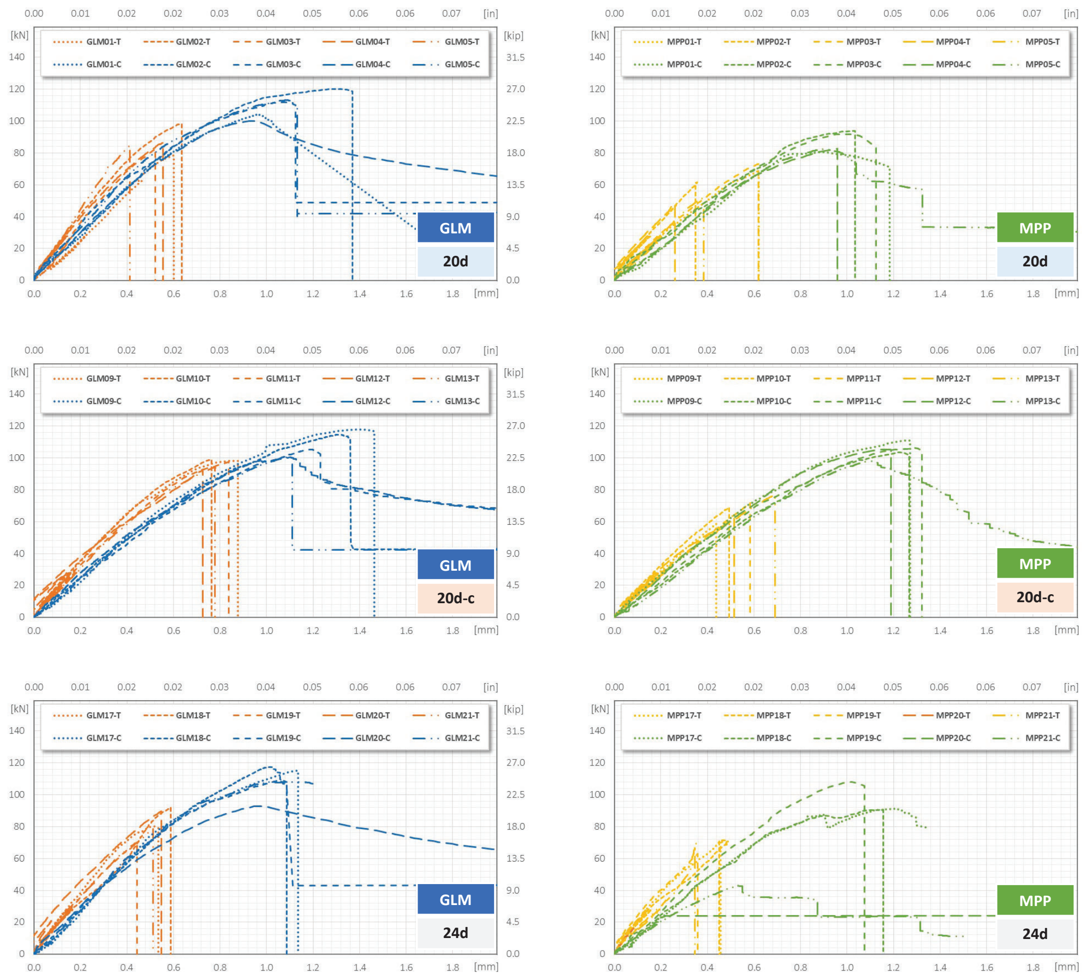

Figure 4: *Load-slip graphs*

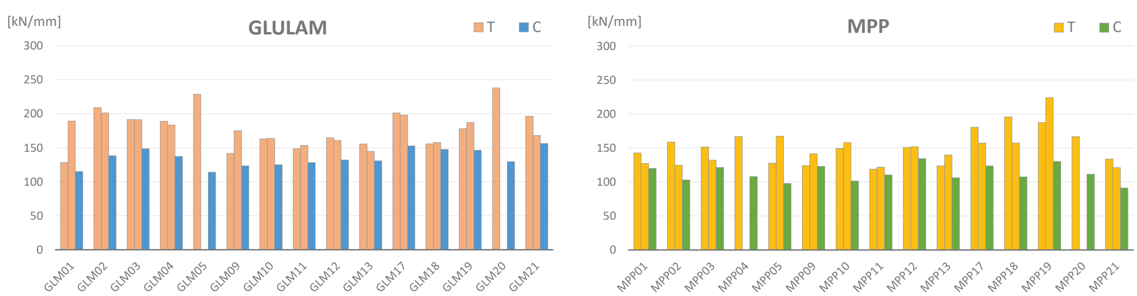

Figure 5: *Slip modulus*

3 RESULTS AND DISCUSSION

A total of sixty tests have been performed in this campaign. Load-slip graphs for each specimen are depicted in Figure 4. For the tensile tests, only the graphs of the failed end are shown. Based on the load-slip data, the slip modulus (k_s) was calculated in the range between 7 kN and 14 kN, which represented 10% and 40% of F_{est} = 70kN. For the tensile tests, the slip modulus was determined for both ends. The values of k_s for each specimen are illustrated in Figure 5.

https://doi.org/10.52202/069179-0173

The statistics for each test series, including the maximum load (F_{max}), the slip modulus (k_s), and predominant failure modes are shown in Table 2 for glulam and in Table 3 for MPP. The mean values and CoV in parentheses are shown for F_{max} and k_s. The moisture content at test and the specific gravity (oven dry mass / oven dry volume) of the specimens are given in Table 4. Typical failure modes of GIR in glulam and in MPP are illustrated, respectively, in Figures 6 and 7, where the top row shows the failures in tension and the bottom shows the failures in compression.

Table 2: *Summary of test results for GIR in DF glulam*

Series	Load direction	F_{max} [kN]	k_s [kN/mm]	Predominant failure mode
20d	Tension	86.4 (8.4%)	190 (14%)	Splitting
	Compression	110 (7.2%)	131 (12%)	Splitting
20d-c	Tension	96.3 (2.9%)	157 (6.6%)	Pull out
	Compression	108 (7.4%)	128 (2.9%)	Push in
24d	Tension	83.7 (13%)	187 (14%)	Splitting
	Compression	109 (8.9%)	146 (7.1%)	Splitting

Table 3: *Summary of test results for GIR in MPP*

Series	Load direction	F_{max} [kN]	k_s [kN/mm]	Predominant failure mode
20d	Tension	60.8 (18%)	144 (12%)	Splitting
	Compression	86.3 (7.0%)	110 (9.5%)	Splitting
20d-c	Tension	67.8 (11%)	138 (11%)	Splitting
	Compression	105 (4.5%)	115 (12%)	Splitting
24d	Tension	68.7 (4.9%)	169 (19%)	Splitting
	Compression	96.7 (29%)	115 (12%)	Splitting

Table 4: *Moisture content and specific gravity (mean and SD)*

Series	Glulam		MPP	
	MC	SG	MC	SG
20d	13.2% (0.6%)	0.519 (0.049)	9.0% (0.5%)	0.531 (0.020)
20d-c	13.1% (0.5%)	0.504 (0.021)	9.4% (0.4%)	0.549 (0.012)
24d	12.8% (0.3%)	0.528 (0.018)	8.6% (0.5%)	0.511 (0.017)

From the test results on GIR in glulam (Series GLM), the following observations were made. The GSA GIR joints (Series 20d-c) showed the highest strength, with the least variability and, most importantly, predominantly favourable failure modes – pull out in tension and push in – in compression. The strength of joints appeared to be independent of the specific gravity of wood. The GIR joints without the constriction zone were somewhat stiffer, but they were weaker and all, but one specimen, failed by wood splitting when loaded in tension. When loaded in compression, all GIR joints in glulam showed a higher resistance than in tension; the maximum load and the variability were independent on the configuration. No buckling of rods was observed, although the maximum loads approached or exceeded the minimum specified yield load of steel.

GIR joints in MPP failed by splitting in 100% of the tests, which led to a lower resistance than expected. The resistance and the stiffness of these joints in tension and in compression were lower than in glulam.

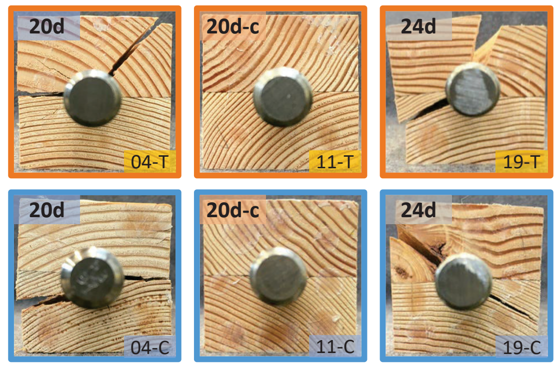

Figure 6: *Typical failure modes of GIR in glulam*

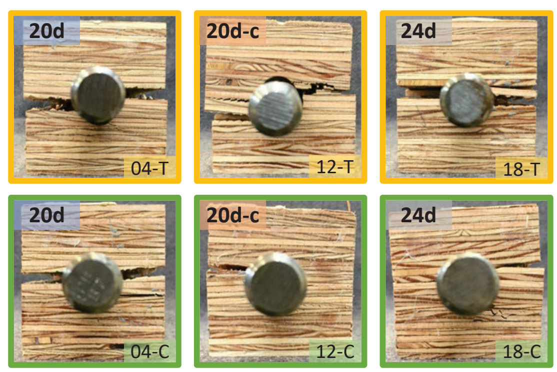

Figure 7: *Typical failure modes of GIR in MPP*

After the tests, each specimen was cut open along the rod to inspect the quality of the manufacturing and further investigate the failure modes and potential reasons for the splitting. It was established that in many cases rods were installed with an inclination of the axis up to 1.6° from the axis of the wood member. Not optimal drilling technology (Auger Bit) is considered as a reason for this misalignment of some predrilled holes in the wood member. Examples are shown in Figure 8. The deviations of the axis were especially frequent in the MPP specimens. These deviations resulted in the eccentricity of the load application, which may have exacerbated the propensity of wood for splitting. However, the investigation showed that the GIR with the largest inclination between the two rods in the specimen did not always fail first in the tension test.

Figure 8: *Inclination of rods in the specimens*

4 CONCLUSIONS

The presented test campaign served for the development and validation of the first edition of the acceptance criteria ICC-ES AC526 for factory installed glued-in rods in wood structural elements for the use in mass timber construction in North America [15]. The developed test procedure and setup with three displacement sensors allowed evaluating the strength and stiffness of GIR in mass timber with high precision. The static test results clearly demonstrated the benefits of recessing the effective bond length in GIR joints to increase the structural efficiency of timber connections. It was demonstrated that resistance in compression was not compromised, and the GIR joints reached the maximum loads without lateral buckling of the rods. It was also observed that the deviation of the rod from the axis of the wood member during fabrication exacerbates the propensity of wood for splitting. Lastly, it was evident that the tested MPP specimens were undersized and were susceptible to splitting; therefore, aiming for a similar resistance per rod, GIR joints in MPP would require larger spacing and edge distances in real structural applications.

ACKNOWLEDGEMENT

Jean Ouellet and Félix Pedneault, technicians at the Renewable Materials Research Centre (CRMR) at Laval University, developed the test setup. Étienne Lapointe conducted the tests at FPInnovations laboratory in Québec City.

REFERENCES

[1] E. Gehri. Glued-in anchors – requirements and applications. In: Internationales Holzbau Forum, Garmisch-Partenkirchen, Germany, 2009.

[2] С. Б. Турковский, А. А. Погорельцев, И. П. Преображенская. Клееные деревянные конструкции с узлами на вклеенных стержнях в современном строительстве (система ЦНИИСК). Москва, РИФ «Стройматериалы». 2013. (in Russian)

[3] CP382. Glued laminated timber structures with glued-in rods. Design Methods. Moscow, RF, 2018.

[4] ETA-19/0752. GSA Technologie. Glued-in rods for timber connections. Austrian Institute for Construction Engineering. 2020.

[5] Avis Technique 3.3/19-986_V1. Goujons collés RBF. CSTB. 2019.

[6] ETA-19/0194. Hilti HIT-RE 500 V3. Glued-in rods for timber connections. Austrian Institute of Construction Engineering. 2019.

[7] ETA-Z-9.1-705. 2K-EP-Klebstoff WEVO-Spezialharz EP 32 S mit WEVO-Härter B 22 TS zum Einkleben von Stahlstäben in Holzbaustoffe. Deutsches Institut für Bautechnik. 2021.

[8] ETA-Z-9.1-778. 2K-EP-Klebstoff GSA-Harz und GSA-Härter für das Einkleben von Stahlstäben in Holzbaustoffe. Deutsches Institut für Bautechnik. 2017.

[9] ETA-9.1-791. Verbindungen mit faserparallel in Brettschichtholz eingeklebten Gewindestangen für den Holzbau. Deutsches Institut für Bautechnik. 2021.

[10] ETA-Z-9.1-896. 2K-PUR Klebstoff LOCTITE CR 821 PURBOND zum Einkleben von Stahlstäben in tragende Holzbauteile. Deutsches Institut für Bautechnik. 2020.

[11] EOTA EAD 130006-00-0304. Glued-in rods for timber connections. European Assessment Document. European Organisation for technical assessment. 2019.

[12] CEN-EN 17334. Glued-in rods in glued structural timber products - Testing, requirements and bond shear strength classification. European Committee for Standardization. 2021.

[13] EOTA TR 070:2019-10. Design of glued-in rods for timber connections. Technical Report. European Organisation for technical assessment. 2019.

[14] CEN/TC 250/SC 5 prEN 1995-1-1:20XX. Eurocode 5: Design of timber structures — Common rules and rules for buildings — Part 1-1: General. 2022.

[15] ICC-ES AC526. Acceptance criteria for factory installed glued-in rods in wood structural elements. June 2022.

[16] ASTM F1554-18. Standard Specification for Anchor Bolts, Steel, 36, 55, and 105-ksi Yield Strength. ASTM International, West Conshohocken, PA, United States. 2018.

https://doi.org/10.52202/069179-0173

[17] APA PR-L325. FRERES Mass Ply Panel (MPP) and Mass Ply Lam (MPL) Beams and Columns. Freres Lumber Co., Inc. APA – The Engineered Wood Association, Tacoma, WA. 2021.
[18] ISO 6891:1983. Timber structures — Joints made with mechanical fasteners — General principles for the determination of strength and deformation characteristics. Reapproved in 2021.
[19] ASTM D2395-17. Standard Test Methods for Density and Specific Gravity (Relative Density) of Wood and Wood-Based Materials. ASTM International, West Conshohocken, PA, United States. 2017.